Effect of Temperature on Dynamic Rheological Properties of Uncured Rubber Materials in Both the Linear and the Nonlinear Viscoelastic Domains

Jean L. Leblanc

UPMC—Paris-Sorbonne Universités, Polymer Rheology and Processing, 60, rue Auber—94408 Vitry-sur-Seine, France

Received 16 December 2011; accepted 13 February 2012
DOI 10.1002/app.37006
Published online in Wiley Online Library (wileyonlinelibrary.com).

ABSTRACT: Investigating how rubber materials are affected by strain and strain rate (or frequency) in the room-to-curing temperature range allows to fully characterize them not only with respect to their processing behavior but also in view of their likely performances after vulcanization. Using a closed cavity dynamic rheometer, the adequate test protocols and data treatment, three gum elastomers, and three carbon black filled compounds were investigated in the 60–180°C range. The article describes the test protocol and the associated data treatment that were developed to document the effects of strain and temperature in both the linear and the nonlinear domains. Complex modulus G^* and third relative torque harmonic variations with strain amplitude and temperature are reported and discussed in details. A set of relatively simple mathematical equations are demonstrated to offer the possibility to summarize large quantities of experimental data through a limited number of parameters whose physical meaning can be explained with respect to known aspects of polymer and rubber sciences. © 2012 Wiley Periodicals, Inc. J Appl Polym Sci 000: 000–000, 2012

Key words: activation energy; elastomers; fillers; rheology; modulus

INTRODUCTION

It is well known that temperature effects are somewhat different in the linear and nonlinear viscoelastic domains of polymers. Rubber materials are generally amorphous polymers so that in the room temperature range, they are on their rubbery plateau, largely above their glass transition temperature. Although they are generally processed above 100°C, no phase change occurs during processing contrary to most thermoplastics. It follows that the processing (temperature) window of elastomers coincides with their usage window, and this is the main reason why these materials must be vulcanized to obtain useful objects.

Most rubber processing operations occur in a relatively wide shear rate range, typically 100–1000 s^{-1} and in the room-to-curing temperature range.[1] Either in terms of shear rate or of strain ranges, all processing addresses the nonlinear viscoelastic properties of the material. In this respect, however, standard processing test methods are far to give adequate information.[2] Rheological properties are usually considered through the (single rate) Mooney viscosity test.[3,4] Curing properties are assessed through the so-called Mooney scorch test[3,4] and through vulcametry tests with either the Oscillating Disc[5,6] or the Moving Die[7] rheometers. Vulcanization properties do not belong directly to the rheological behavior *per se* but rather to the chemical virtues of the curing system, so that how some conveniently chosen rheological properties do vary in the room-to-curing temperature range and in the linear-to-nonlinear viscoelastic region is really the key information that should be obtained. In principle, capillary rheometry would be an attractive method to document the medium and high-shear rate behavior of rubber materials but, practically, it is rarely used owing to its slowness and tediousness, particularly if the behavior must be documented over a temperature range. Dynamic rheometry techniques are therefore techniques of choices, but rubber materials are generally so stiff that they must be evaluated with special rheometers and closed-cavity dynamic torsional instruments have been proved over the last decades to be particularly suitable.

How temperature variations affect the dynamic response of rubber materials in both the linear and the nonlinear viscoelastic domains is thus the subject of this report. A strain sweep (SS) test protocol and the associated data treatment will be described so that by performing it at various temperatures in the 60–180°C range, an overall knowledge of the strain

Correspondence to: J. L. Leblanc (jean.leblanc@ifoca.com).

TABLE I
Test Materials; Gum Elastomers

Material	Sample name	Typical features	Supplier	M_W (g/mole)	Mooney viscosity ML (1 + 4)
EPDM	EPDM2504	57.5 ± 3.0% ethylene 4.7 ± 0.6% ENB	Exxon Mobil	186,000	25 ± 4 at 125°C
BR	BR1220	≈96% *cis*-1,4-polybutadiene	Shell	220,000	41–49 at 100°C
SBR	SBR1500	Emulsion SBR 23.5% Styrene	Lanxess	510,000	50 at 100°C

ENB, ethylene norbornene.

and temperature effects on the dynamic rheology of rubber systems may be obtained. Results on various gum elastomers (ethylene-propylene-diene monomer rubber, EPDM; *cis*-1,4-polybutadiene, BR; styrene-butadiene rubber, SBR) and several carbon black filled compounds will be reported and discussed in details by making use of adequate fitting equations.

EXPERIMENTAL

Test materials

SBRs are by far the most important synthetic elastomers with annual world-wide consumption in the 4 millions tons range, and emulsion SBR1500 is the most common grade because its properties are not far from those of natural rubber, except it has no strain-induced crystallization capabilities. SBR 1500, with an average 23% weight styrene and a Mooney viscosity $ML(1 + 4)_{100°C} = 45–55$, is a standard product in the rubber industry and was therefore selected for this study. Experiments as described below were performed on a series of gum elastomers commercially available in France (Table I) and a series of carbon black filled compounds (Table II). Carbon black SBR 1500 compounds, as described in Table II, were prepared in a Haake Rheocord 90 laboratory mixer, equipped with a 300 cm^3 chamber and Banbury type rotors. Rotors rate was 40 RPM, fill factor 0.7 and a dead weight of 5 kg was used to close the chamber. All mixing operations started at 80°C. The procedure was as follows: with the rotors running and the temperature stabilized, the rubber load, cut in small pieces, was first introduced and masticated for 30 s; then half the carbon black content (if any), the zinc oxide, and the stearic acid were introduced with the assistance of the ram, then the rest of the compounding ingredients were added and the mixing maintained until 5 minutes were elapsed. The rotors were stopped, the mixer opened and the collected batch was passed 10 times without banding on a two-rolls mill so that a sheet was obtained, which was left to cool down on a stainless steel bench. The overall mixing energy for each compound was obtained by integration of the recorded torque vs. time curve. Compounds were stored in darkness at room temperature.

TABLE II
Test Materials; Rubber Compounds

		N330 carbon black		
Material	*Sample name*	phr	**Vol. fraction**	Mixing energy (MJ/m^3)
SBR[a]	SBR00	0	0	423.6
	SBR10	10	0.0431	526.7
	SBR50	50	0.1836	732.5

[a] Formulation (phr): rubber, 100; carbon black, variable; naphthenic oil, 5; zinc oxide, 5; stearic acid, 3; trimethylquinoline, polymerized (TMQ), 2; *N*-isopropyl-*N*′-phenyl-*p*-phenylene diamine (IPPD), 1.

Closed cavity torsional dynamic rheometers

A fast and convenient technique to investigate the nonlinear viscoelastic response of polymer materials consists in performing SS tests from the lowest up to the highest strain amplitude either permitted by the instrument or before boundary conditions between the sample and the test gap walls cease to be optimal. With high-molecular weight or highly stiff (molten) polymer systems, investigations with traditional open gap (e.g., cone-and-plate or parallel disks) rheometers are at best limited to the medium amplitude range, i.e., up to 100%, before peripheral edge fracture appears.[8] With many polymer systems of industrial importance, only closed cavity torsional dynamic rheometers allow obtaining reproducible and meaningful results under large amplitude oscillatory strain (LAOS) conditions. These instruments are nowadays commercially available, e.g., the "Rubber Process Analyzer", RPA 2000®, the "Production Process Analyzer", PPA® (Alpha Technologies, now a division of Dynisco LLC, Franklin, MA), the D-RPA 3000 (MonTech Werkstoffprüfmaschinen GmbH, Buchen, Germany). All these instruments have a sealed test chamber with a reciprocal biconical geometry with a low opening angle of 0.125 rad and 20 small grooves (9.8 × 1.9 × 0.635; length × width × depth; mm) to prevent slippage (Fig. 1). The cavity must be fully loaded and a fluoroelastomer seals system insures tightness of the test cavity, which is kept closed under 6 MPa pressure during experiments.

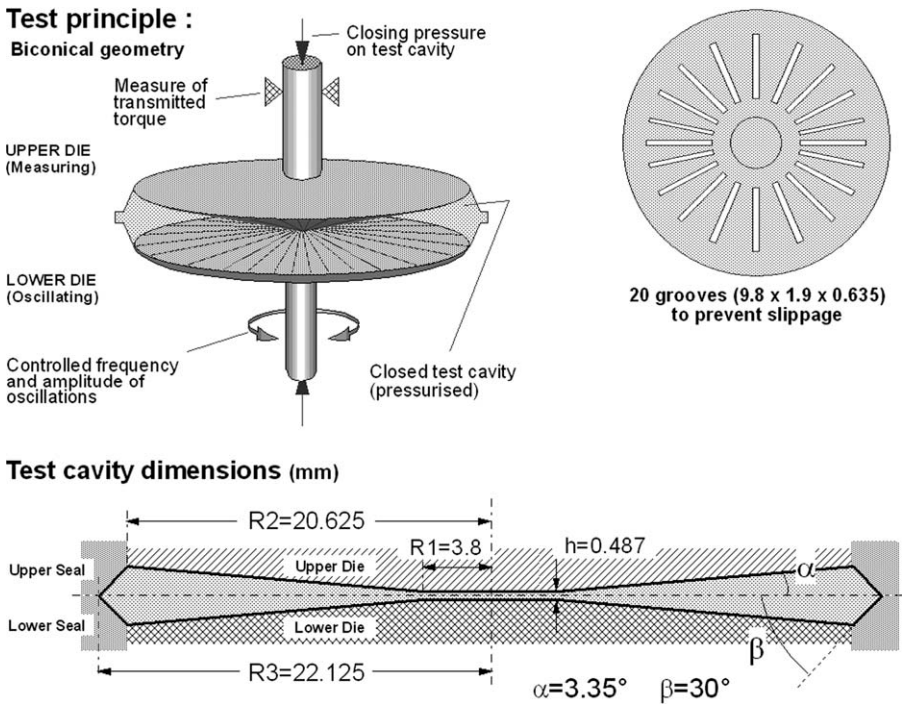

Figure 1 Test principle of closed cavity torsional dynamic rheometers and typical cavity geometry and dimensions.

Strictly speaking, in closed cavity torsional rheometers, the theoretical requirements for simple shear flow are not fully met in terms of peripheral boundary conditions. For instance, the sample edge surface is expected to be spherical with the open gap cone-and-plate system and cylindrical with parallel disks. This is obviously not the case with the test cavity geometry described in Figure 1. Indeed, numerical simulation has shown that in the closed cavity rheometer, there is a region of high-shear rate at the bottom part of the edge, where the oscillating lower die is in contact with the fixed seal. Conversely, at the top part of the edge, where the measuring upper die is in contact with the seal, the shear rate is smaller than the bulk value. However, if the overall flow pattern in the test cavity is considered, such peripheral effects appear relatively not significant, with deviation less than 10% with respect to theory. An experimental demonstration that the peripheral fixed boundary has negligible effect was provided by comparing tests made on a model polystyrene with a closed cavity rheometer and other dynamic torsional rheometers (with an open rim): deviations of less than 5% on both G' and G'' were observed.[9] Furthermore, Debbaut and Burhin[10] used a multimode Giesekus model to describe the nonlinear rheological behavior under large amplitude oscillation of a high-density polyethylene in such a closed biconical cavity and found that, although the kinematics deviate from those of simple shear flow, the total harmonic distortion is very similar. It may therefore be concluded that the technological constraints imparted by the closed biconical cavity are quite negligible in regard to the possibility to perform reproducible and significant LAOS tests on highly stiff, viscous, and elastic materials, otherwise difficult, if possible to study with conventional rheometers.

SS test protocol

All hereafter reported experiments were performed with an RPA 2000, suitably updated for Fourier Transform rheology, essentially by capturing strain and torque signals, using a 16-bit electronic analogic-digital conversion card and resolving them into their harmonic components by means of appropriate calculation algorithms. Details on the RPA modification for FT rheometry and on the data treatment have already been published.[11] SS tests in the 0.5–68.0 deg range (6.98 to 949.46%) at fixed frequency (0.5 Hz; 3.14 rad/s) were performed at various temperature in the 60–180°C range. In all cases, a sample of the test material was cut out of an approximately 2.5 mm thick piece, either a slice cut from the bale (gum samples) or a milled sheet (compound samples), by using a circular die of 4 cm diameter. The sample weight was controlled so that its volume was around 3.1 cm^3. The sample was loaded in the rheometer cavity, previously thermally stabilized at 110°C. After closing the test cavity, the temperature is decreased (or increased) from 110° to the selected test temperature and maintained for 3 min, then a gentle 0.2 deg strain at 1 Hz is applied for 30 sec

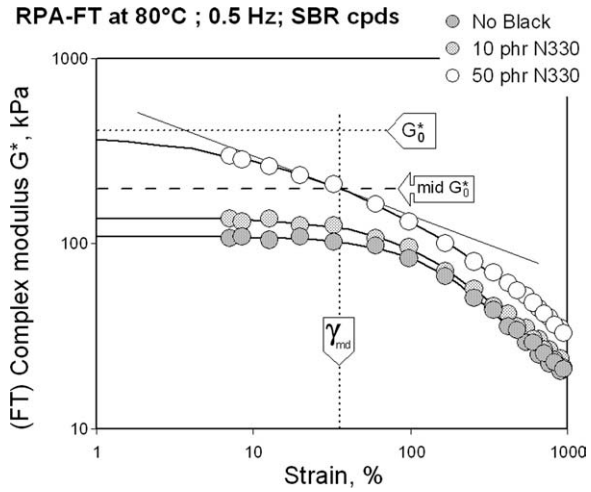

Figure 2 Typical complex modulus vs. strain amplitude variations of SBR compounds at 80°C, 0.5 Hz; data were fitted with eq. (1); a few information extracted from the model are shown in the case of the 50 phr carbon black filled compound.

and followed by a resting period of 2 min. SS experiments (0.5 Hz) are then performed. At least two samples of the same material are tested in each test conditions so that 20 strain steps were investigated at all test temperatures.

Data treatment and analysis

According to the SS test protocol described above, RPA-FT experiments and data treatment yield essentially two types of information, which reflects how the main torque component, i.e., TH(ω), and the relative torque harmonics, i.e., $TH(n/1) = TH(n\omega)/TH(\omega)$ vary with strain amplitude. The main torque component is converted in complex modulus according to $G^*(\omega) = Q \times \frac{TH(\omega)}{\gamma}$, where Q is a conversion factor that depends on the torque transducer, the analog-to-digital signal conversion system, and the unit used for G^* (here kPa). G^* vs. strain curves generally exhibit the most familiar picture of a plateau region at low strain, then a typical strain dependence. $G^*(\gamma)$ data are conveniently fitted with a four parameters model, i.e.:

$$G^*(\gamma) = G_f^* + \left[\frac{G_0^* - G_f^*}{1 + \left(\frac{\gamma}{\gamma_{md}}\right)^B}\right] \quad (1)$$

where γ is the set strain amplitude, G_0^*, the modulus in the linear region, G_f^*, the final modulus, γ_{md}, the strain for reaching the midmodulus value, i.e., $(G_0^* + G_f^*)/2$, and B, a parameter related to the strain sensitivity of the material. Figure 2 shows typical results on SBR compounds at 80°C. As can be seen, the linear viscoelastic plateau is clearly observed in the cases of the unfilled and the 10 phr carbon black compounds. Equation 1 perfectly fits experimental data in all cases, even if for the highest filled compound, the linear modulus G_0^* is a (largely) extrapolated value. Summarizing experimental data by means of eq. (1) allows various interesting information to be extracted by exploiting the mathematical virtues of the model. For instance, the first derivative of eq. (1) allows calculating the slope at any strain value. The straight line that can be drawn using the slope at γ_{md} and that passes through the point $[(G_0^* + G_f^*)/2; \gamma_{md}]$ is also interesting because its intercept with G_0^* determines a strain amplitude that is an unambiguous limit between the linear and the nonlinear viscoelastic regions.

When submitted to a harmonic (i.e., cyclic) strain $\gamma(t)$ a pure, homogeneous viscoelastic material gives a stress response $\sigma(t)$, which is also harmonic, but except in the limit of (infinitesimally) small strain, stress and strain are generally not simply proportional. If the applied cyclic strain does correspond to a simple sinusoidal definition, e.g., $\gamma(t) = \gamma_0 \sin(\omega t)$, where γ_0 is the maximum strain amplitude, ω, the frequency (rad/s), and t the time (s), one can thus expect the general stress response to correspond to summation of terms, i.e., $\sigma(t) = \sum_i \sigma_i \sin(i\omega t - \delta_i)$ where the δ_i terms allow accounting for an out-of-phase retard of the stress component σ_i with respect to the applied strain. In the limit of infinitesimally small strains, such a series is expected to reduce to only the first term when the material is exhibiting a so-called linear viscoelastic response.[12] This means that, beyond the linear viscoelastic region, harmonics may be expected in the stress response, for instance in the torque signal if the torsional shear method is used.

Odd torque harmonics become significant as strain increases and are therefore considered as the nonlinear viscoelastic "signature" of tested materials. So far, no theory is really available that would allow to interpret specific harmonics in terms of particular features of molecular structure or specific features of a constitutive equation, despite a few promising attempts as recently reviewed by Hyun et al.[13] Experiments on many polymer systems have however shown that the manner odd torque (or stress) harmonics significantly increase with higher strain amplitude can be considered as a typical nonlinear viscoelastic "signature" of tested materials. Numerous RPA-FT experiments on various pure, unfilled polymers have shown that relative torque harmonics [here noted, $TH(n/1)$ and expressed in %] vary with strain amplitude in such a manner that an initial sigmoid curve appears bounded by a simple linear variation at high strain. Accordingly, the following equation was initially developed to treat results obtained on a series of gum natural rubbers[14] and

found applicable to many systems so far tested, except highly filled rubber compounds,[15] i.e. :

$$\mathrm{TH}(\gamma) = (\mathrm{TH}_0 + \alpha\gamma) \times [1 - \exp(-C\gamma)]^D \quad (2)$$

where γ is the set strain magnitude, TH_0, α, C, and D parameters of the model. TH stands for any relative harmonic, i.e., TH(3/1), TH(5/1), etc. Equation 2 was also found applicable to the sum of all (measurable) torque harmonics, called the total torque harmonic content (TTHC), $\mathrm{TTHC} = \sum \mathrm{TH}(n\omega/\omega)$. The first right member in eq. (2), i.e. $(\mathrm{TH}_0 + \alpha\gamma)$, expresses a linear variation of harmonics in the high-strain region, whereas the member $[1-\exp(-C\gamma)]^D$ describes the development of the nonlinear viscoelastic response. TH_0 is the extrapolation towards $\gamma = 0$ of the high-strain linear variation and α is the slope of the asymptotic high-strain behavior. The member $[1-\exp(-C\gamma)]^D$ corresponds to a sigmoidal curve that goes asymptotically to 1, whatever the values are for C and D. However, D is clearly associated with the extent of the linear region (where torque harmonics must go asymptotically to zero), although C reflects the strain sensitivity, in other words, the manner the material goes from the linear to the nonlinear region. The position of the maximum of the first derivative is a critical strain of the material that corresponds in fact to $\frac{\ln D}{C}$.

Figure 3 shows typical torque harmonics as measured on gum EPDM and SBR 1500 at 140°C, 0.5 Hz. Measured third TH(3/1) and fifth TH(5/1) relative torque harmonics are given, and the TTHC and their respective fitted curves are drawn. The TTHC curve is the envelope of all the torque harmonics and the third harmonic is the most intense one and therefore the dominating component in TTHC. The contribution of the fifth and (expectedly) upper harmonics becomes however quite significant when the strain amplitude is sufficiently large.

In eq. (2), the physical meaning of parameters TH_0 and α is obvious: high-strain harmonics are asymptotic to a straight line whose slope is α and TH_0 is the zero strain intercept. If indeed, the occurrence of a plateau is visible in the experimental strain window, parameter α will be found so small that sometimes it can readily be assigned a zero value. In such a case, TH_0 is a plateau value, that can be considered as the maximum degree of nonlinearity for each harmonic and the first right member of eq. (2) reduces to TH_0. Such a behavior has been observed in a few instances but not always. According to Wilhelm et al.,[16] for a Newtonian fluid, relative harmonics TH(n/1) can never be higher than $1/n$; for instance, the relative harmonic TH(3/1) cannot be higher than 1/3. Polymers are non-Newtonian fluids so that theoretical considerations for Newtonian fluids do not apply but, practically, relative torque harmonics approaching the theoretical maximum

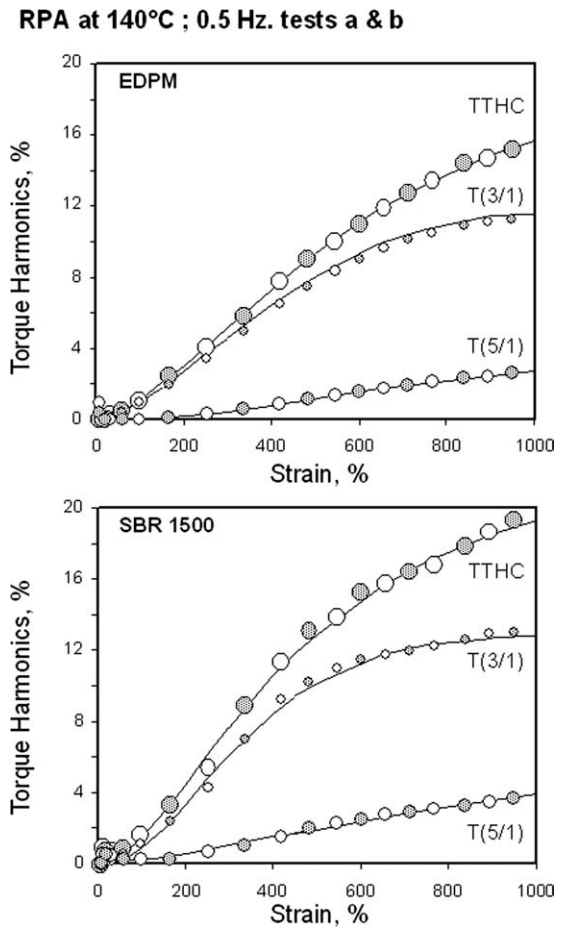

Figure 3 Typical torque harmonics data as measured on gum EPDM and SBR 1500 at 140°C, 0.5 Hz; the third TH(3/1), the fifth TH(5/1), and the TTHC are shown, as well as the respective fitted curves.

$1/n$ have never been observed and many experimental results suggest that the high-strain behavior might be typical of the material under investigation, in the conditions of the test. The development of the nonlinear response is accounted for by parameters C and D in the second right member of the equation. Parameter D somewhat reflects the extent of the linear viscoelastic region (i.e., where essentially no harmonics are detected), whereas parameter C indicates the strain sensitivity of the nonlinear character. As the strain γ is smaller and smaller, eq. (2) corresponds to asymptotically zero harmonics, as expected in the linear viscoelastic region and thus in complete agreement with theory.

Filled materials generally exhibit a more complex variation of torque harmonics with strain amplitude such that a "bump" appears in the linear-to-nonlinear transition region. A more complicated version of eq. (2) has consequently been developed that yields an adequate fit of experimental data in the overall strain region.[15] This special model for filled materials was proposed by considering that there is superimposition of two responses (to dynamic strain):one

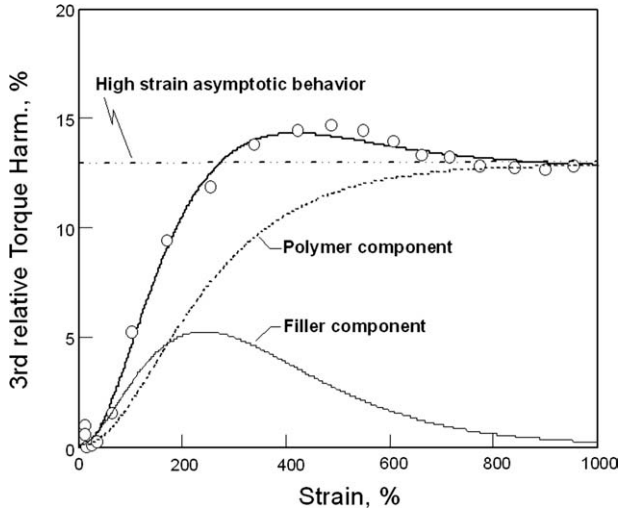

Figure 4 Typical third relative torque harmonic vs. strain data as measured on a SBR1500/50phr N330 carbon black compound at 0.5 Hz, 180°C and fitted curve (bold line); the three component of eq. (3) are indicated.

qualitatively common to all "pure" (or virgin, unfilled) polymers and readily well modeled with eq. (2) above, and a curve that passes through a maximum at a typical strain value and expresses the "filler response" to dynamic strain of increasing amplitude. The physical reasoning in selecting the most appropriate mathematical model for the filler response was based on two major aspects: (1) interactions between the rubber and the filler phases enrich the harmonic response of the system at the onset of the nonlinear region; and (2) above a critical strain, such interactions begin to be modified so that their effects vanish at sufficiently large strain amplitude.

The torque harmonic vs. strain model for filled systems corresponds to the following equation:

$$\mathrm{TH}(\gamma) = (\mathrm{TH}_0 + \alpha \cdot \gamma) \cdot \Big[(1 - \exp(-C \cdot \gamma))^D + W_1 \cdot (W_2 \cdot \gamma)^{(W_3 - 1)} \cdot \exp(-W_2 \cdot \gamma)^{W_3}\Big] \quad (3)$$

where γ is the set strain amplitude and TH(γ) stands for any relative torque harmonic, i.e. TH($n\omega/1\omega$), and also for the so-called TTHC [i.e. $\sum \mathrm{TH}(n\omega/1\omega)$]. The S-shape polymer response is modeled with only two parameters, C and D and the physical meaning of the parameters of the equation is understood as follows (see Fig. 4 for a pictorial illustration):–the first (right) member describes the asymptotic high-strain behavior; this member multiplies the sum of the two last right members of the equation:

$$(\mathrm{TH}_0 + \alpha\,\gamma) \quad (3a)$$

–the second member describes the polymer response in the linear-to-nonlinear transition region (one can also call it the polymer matrix component); this member corresponds to a S-shape curve that goes from 0 to 1:

$$(1 - \exp(-C\,\gamma))^D \quad (3b)$$

–the third member describes the filler response (it can also be called the filler component) and corresponds to a curve that passes through a maximum:

$$W_1\,(W_2\,\gamma)^{W_3 - 1} \exp(-W_2\,\gamma)^{W_3} \quad (3c)$$

Parameters in eq. (3a and b) have exactly the same physical meaning as in eq. (2), i.e., TH_0 is the extrapolation toward $\gamma = 0$ of the high-strain linear variation and α is the slope of the asymptotic high-strain behavior, C is associated with the strain sensitivity in the linear-to-nonlinear transition region and D reflects the extent of the linear region (where torque harmonics must go asymptotically to 0).

The filler component [i.e., eq. (3c)] expresses the idea that the filler effect on viscoelastic nonlinearity passes through a maximum because an influential filler structure is first inducing an additional nonlinearity as strain increases, then is destroyed (or dislocated) above a critical strain, to eventually cease to be effective when the strain amplitude is sufficiently large. The appropriate mathematical form of the filler response was developed with respect to the well-known Weibull analysis* and its probability density function of failure modes in the course of any (complex) industrial process. The logics behind the Weibull analysis was transposed to the torque harmonics variation with strain magnitude of filled systems by considering that, because of strong interactions between the viscoelastic matrix and the discrete phase, a kind of soft composite network is embedded in the (free) rubber phase. The soft composite consists of the carbon black particles in interaction with the bound rubber, in agreement with well-established views.[17] It follows that there are filler-dependent additional harmonics in the medium strain range, which enhance the ongoing nonlinear response of the matrix, then as strain further increases, filler–polymer interactions decrease and eventually vanish in such a manner that, for a sufficiently high-strain amplitude, essentially the high-strain response of the polymer plays yet a role.[15]

Physical meaning for the W_i parameters in eq. (3c) can be sought with respect to their mathematical virtues. First, W_3 must be larger than 1 for a maximum to occur but the sharpness of the maximum strongly

*Named after the Swedish engineer Waloddi Weibull (1887–1979) who used a special family of distribution functions for reliability analysis in metallurgical failure modes.

TABLE III
Complex Modulus vs. Strain Data on Gum Rubbers; Fit Parameters of Eq. (1)

	Temperature (°C)				
Material	60	80	100	140	180
EPDM 2504					
G^*_0	272.28	168.76	109.43	53.25	30.18
G^*_f	27.31	16.35	13.92	9.75	5.82
γ_{md}	194.9	194.6	283.8	310.9	326.3
B	1.634	1.508	1.506	1.454	1.323
r^2	0.9981	0.9931	0.9995	0.9994	0.9994
BR 1220					
G^*_0	138.97	123.3	113.3	101.78	105.8
G^*_f	25.64	22.77	21.05	20.94	24.55
γ_{md}	158.9	159.5	151.6	132.5	124.3
B	1.678	1.635	1.610	1.676	1.777
r^2	0.9859	0.9955	0.9983	0.9984	0.9898
SBR 1500					
G^*_0	190.11	134.88	101.8	64.08	46.57
G^*_f	21.74	18.91	16.9	13.82	12.13
γ_{md}	197.0	205.5	199.4	177.0	158.2
B	1.669	1.597	1.559	1.564	1.692
r^2	0.9979	0.9981	0.9991	0.9994	0.9985

decreases when W_3 is larger than 3, second the strain position of the maximum is moving to larger value as W_2 increases, and third the larger W_1, the higher the maximum. One would thus expect the reinforcing character of the filler to be essentially associated with W_1 and W_2, the former likely associated with the filler loading and the latter likely reflecting its reinforcing strength.

RESULTS AND DISCUSSION

Summarizing results through fit parameters

Fourier transform rheometry provides quite a large amount of information that can be conveniently summarized in a small number of significant parameters by fitting experimental data with the models previously described [eqs. (1 and 2) in section 'Data treatment and analysis']. Analyzing the fit parameters makes for an easier comparison between tested materials.

Complex modulus curves were fitted with eq. (1), yielding data given in Tables III and IV. Third harmonic model parameters [eq. (2)] are given in Tables V and VI. As can be seen, the fitting is excellent with r^2 above 0.98, in most cases.

Gum rubber: Complex modulus variations with strain amplitude and temperature

Let us consider first how G^* vs. strain curves vary with increasing temperature. Table III shows that all parameters of eq. (1) generally decrease with increasing temperature, with some differences however that can be assigned to the rubber nature. A first manner to study temperature effects in both the linear and nonlinear regions consists in using eq. (1) and the corresponding fit parameters to recalculate several values of G^* at selected strains so that both viscoelastic domains are considered. By definition G_0^* is the absolute "linear" modulus as it would correspond to an "asymptotic" 0 strain modulus. The so-called mid-modulus value, G_{md}^* is calculated with respect to the critical strain γ_{md} and is in the nonlinear region and a modulus calculated at several 100%, let's say 600%, is in the far nonlinear region. By drawing Arrhenius plots, i.e., $\ln(G^*)$ vs. $1/T$ plots, the temperature effects in both the linear and the nonlinear regions can be quantified with respect to the activation energy, in agreement with the so-called Arrhenius equation, i.e., :

$$G^*(T,\gamma) = G^*(T_0,\gamma) \times \exp\left[\frac{E_a}{R}\left(\frac{1}{T}-\frac{1}{T_0}\right)\right] \quad (4)$$

where T_0 and T are a reference temperature and the test temperature, respectively (in Kelvin); R, the gas constant (8.3145 J/K mole); $G^*(T_0,\gamma)$, the modulus at strain γ and reference temperature T_0, and E_a the activation energy (J/mole), according to the well-known proposal by Svante Arrhenius[18] in 1884. The activation energy is defined as the energy that must be overcome for a process to occur and in the context of this work, it is the energy involved in the dynamic testing within the temperature range considered (i.e., 60–180°C).

As can be seen, for a given sample, the slopes are not exactly equal for the three G^* values considered, meaning thus that strain and temperature effects are not factorable, or in other terms that both effects

TABLE IV
Complex Modulus vs. Strain Data on Rubber Compounds; Fit Parameters of Eq. (1)

	Temperature (°C)					
Material	60	80	100	120	140	180
SBR 1500 No black compound						
G^*_0 (kPa)	183.28	108.94	79.27	62.28	50.24	37.54
G^*_f (kPa)	16.21	12.09	11.89	10.93	9.36	9.21
γ_{md} (%)	163.9	201.2	195.0	187.9	178.9	151.0
B	1.495	1.487	1.477	1.486	1.429	1.565
r^2	0.9864	0.999	0.9989	0.9989	0.9981	0.9979
SBR 1500/10phr N330 compound						
G^*_0 (kPa)	219.41	140.03	92.58	70.44	56.15	41.78
G^*_f (kPa)	15.895	9.53	9.71	9.43	8.28	8.68
γ_{md} (%)	136.0	160.9	169.1	161.7	154.2	127.7
B	1.345	1.225	1.237	1.238	1.208	1.305
r^2	0.9984	0.9969	0.9962	0.9989	0.9993	0.9982
SBR 1500/50phr N330 compound						
G^*_0 (kPa)	483.945	397.97	326.25	260.06	231.63	180.17
G^*_f (kPa)	(−12.74)	(−12.10)	(−6.31)	(−0.13)	1.26	4.86
γ_{md} (%)	41.3	36.5	25.2	21.5	14.8	13.0
B	0.698	0.633	0.587	0.598	0.576	0.627
r^2	0.9947	0.9991	0.9991	0.999	0.999	0.9976

Note that negative G^*_f values reported for the 50 phr black filled compound at certain temperatures have no physical meaning; they just result from the nonlinear fitting process, must be considered as mathematical artifacts but are associated with the mid-modulus strain γ_{md}.

cannot be approach as a mere product of the effect of a parameter times the effect of the other parameter. The activation energy values corresponding to plots in Figure 5 are given in Table VII. As can be seen, for EPDM and SBR, the higher the strain amplitude, the lower the activation energy, but for BR, no significant effect of strain amplitude is seen on E_a.

With respect to eq. (1), a most convenient manner to split temperature and strain effects consists in normalizing both the complex modulus and the strain amplitude. Normalizing the complex modulus by considering the ratio $\frac{G^*(\gamma)}{G^*_0}$ allows taking into consideration the effect of temperature in the linear viscoelastic region. Normalizing the strain amplitude with respect to the critical mid-modulus strain, i.e., the $\frac{\gamma}{\gamma_{md}}$ ratio, allows distinguishing the linear from the nonlinear regions. Figure 6 shows the results of this normalization process in the case of the EPDM sample.

TABLE V
Third Relative Torque Harmonic vs. Strain Data on Gum Rubbers; Fit Parameters of Eq. (2)

	Temperature (°C)				
Material	60	80	100	140	180
EPDM 2504					
$TH(3/1)_0$	11.26	n/a	16.36	12.66	10.44
α	0.0110	n/a	0.0000	0.0000	0.0000
C	0.005	n/a	0.003	0.003	0.004
D	1.800	n/a	1.812	2.101	2.252
R^2	0.9984	n/a	0.9998	0.9996	0.9985
BR 1220					
$TH(3/1)_0$	12.39	11.40	19.61	16.29	14.08
α	0.0000	0.0000	−0.0093	−0.0059	0.0000
C	0.007	0.008	0.004	0.005	0.006
D	3.291	4.635	2.610	2.856	3.252
r^2	0.9916	0.9885	0.9985	0.9960	0.9739
SBR 1500					
$TH(3/1)_0$	19.24	18.18	16.38	13.82	13.58
α	0.0000	0.0000	0.0000	0.0000	0.0000
C	0.003	0.003	0.004	0.005	0.006
D	1.974	2.051	2.341	3.020	3.433
r^2	0.9960	0.9969	0.9969	0.9959	0.9923

TABLE VI
Third Relative Torque Harmonic vs. Strain Data on Rubber Compounds; Fit Parameters of Eq. (3)

	Temperature (°C)				
Material	60	80	100	140	180
SBR 1500 No Black compound					
$TH(3/1)_0$	17.201	13.536	12.865	11.332	10.225
α	0.0008	0.0010	0.0007	0.0014	0.0020
C	0.0044	0.0040	0.0042	0.0055	0.0055
D	6.38	5.77	4.27	5.15	4.31
W_1	6.65	6.21	4.74	3.37	3.30
W_2	0.0018	0.0016	0.0016	0.0019	0.0019
W_3	3.05	3.05	3.06	3.05	3.05
r^2	1.0000	0.9980	0.9990	0.9990	0.9990
SBR 1500/10phr N330 compound					
$TH(3/1)_0$	17.234	13.546	11.832	10.921	10.681
α	−0.0035	0.0010	0.0021	0.0022	0.0018
C	0.0048	0.0040	0.0040	0.0047	0.0055
D	7.18	4.28	3.83	3.74	3.37
W_1	5.12	6.05	6.06	4.64	2.80
W_2	0.0018	0.0017	0.0018	0.0019	0.0019
W_3	3.05	3.04	3.06	3.05	3.05
r^2	0.9980	0.9990	0.9990	1.0000	1.0000
SBR 1500/50phr N330 compound					
$TH(3/1)_0$	13.238	12.401	12.275	11.528	9.998
α	0.0037	0.0036	0.0026	0.0025	0.0035
C	0.0036	0.0040	0.0032	0.0071	0.0088
D	1.57	1.62	1.36	2.65	3.01
W_1	5.68	5.35	6.58	5.63	6.34
W_2	0.0020	0.0022	0.0022	0.0032	0.0032
W_3	3.05	3.05	3.04	3.06	3.05
r^2	0.9980	0.9980	0.9990	0.9980	0.9980

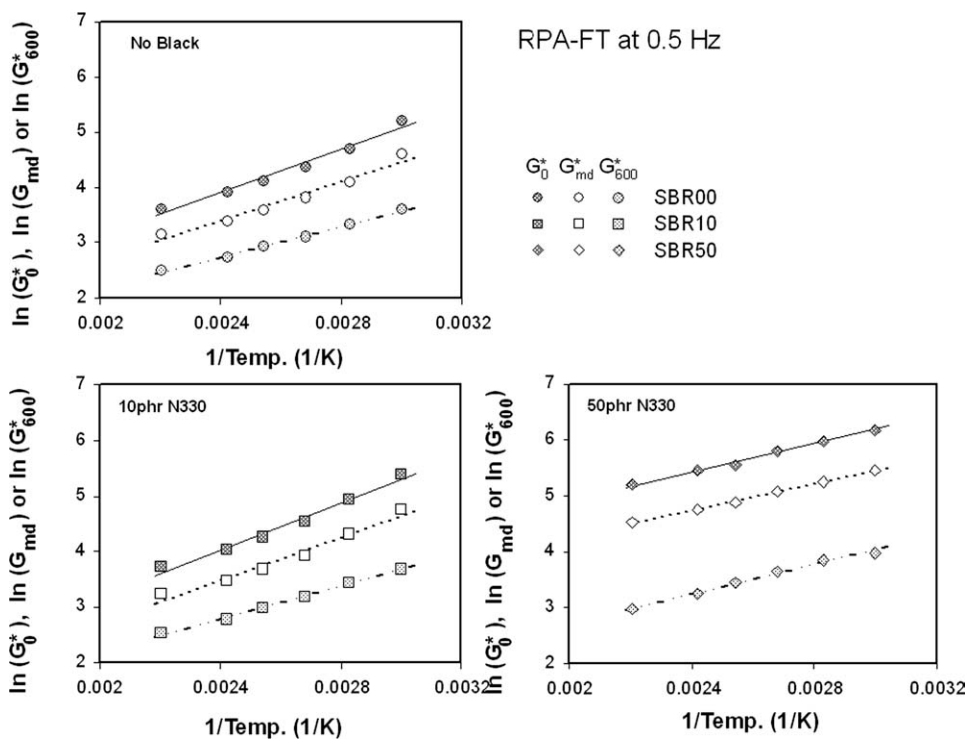

Figure 5 Arrhenius plots of typical complex modulus values that encompass both the linear and nonlinear viscoelastic regions of gum rubbers when tested at constant frequency of 0.5 Hz.

TABLE VII
Gum Rubbers: Activation Energy for G^* (at 0.5 Hz) at Various Strain Amplitudes

	Activation energy (kJ/mole)		
Material	For G^*_0	For G^*_{md}	For G^*_{600}
EPDM2504	23.08	22.15	15.89
BR1220	2.98	2.56	2.65
SBR1500	14.74	13.45	11.31

As expected, data (or fitted curves) at different temperatures merge into a single curve in the linear viscoelastic region. In the nonlinear region, however, a temperature effect clearly superimposes on the strain amplitude's one, so that the higher the temperature, the less sensitive to strain variation is the (normalized) modulus. Figure 7 shows the corresponding graphs for the BR and SBR samples, using only fitted curves for the sake of clarity. As can be seen, all curves for the BR sample fall on a single one, indicating that the strain sensitivity of this material is not significantly affected by temperature in both the linear and the nonlinear regions. The SBR sample calls for the same comments as the EPDM.

In linear viscoelasticity, moduli associated with relaxations are proportional to absolute temperature, and for most polymers but not all (polyethylmethacrylate[19] and polystyrene[20] have been reported to deviate from this rule), all relaxation times and moduli have the same functional dependence on temperature; in such cases, the time-temperature superposition applies. The above figures suggest that relaxation times and moduli of BR do share similar temperature dependency in both linear and nonlinear regions. In the case of EPDM and SBR (both statistical copolymers), increasing temperatures likely shorten relaxation times; hence the lower strain dependent in the nonlinear region as temperature increases.

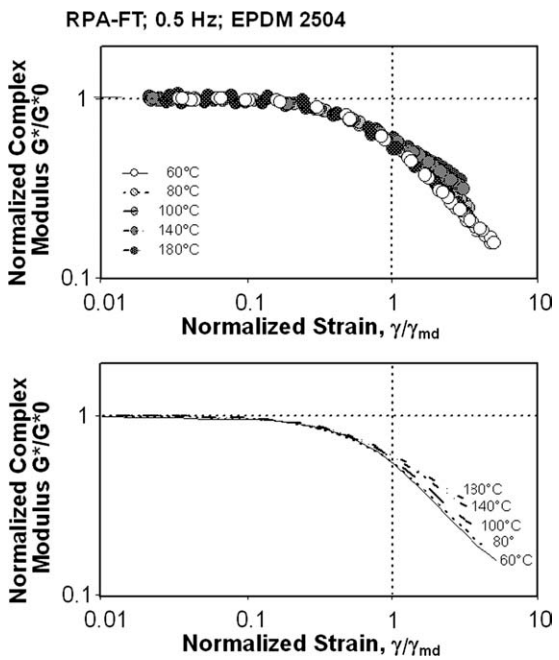

Figure 6 Normalized complex modulus vs. strain data and fitted curves at various temperatures for the EPDM gum sample.

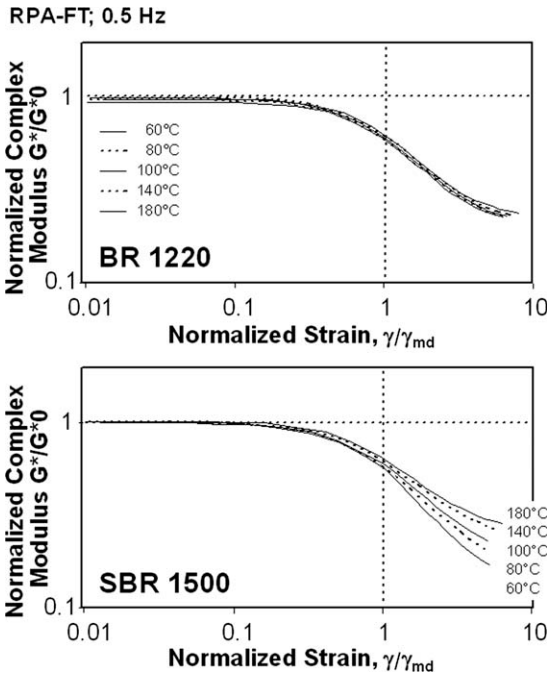

Figure 7 Normalized complex modulus vs. strain curves at various temperatures for the BR and SBR gum samples.

Filled compounds: Complex modulus variation with strain amplitude and temperature

Results with carbon black filled SBR compounds are analyzed using the same approach as above. Three complex modulus values, i.e., G_0^*, G_{md}^* and $G_{600\%}^*$, are either extracted or calculated from fit parameters given in Table V, in order to consider the linear and the nonlinear viscoelastic regions. Note however that, with the highly filled compound SBR50, the linear region is out of reach of the experimental window, so that the "linear" modulus G_0^* is a very far extrapolated data that might be hypothetical (see Fig. 2 above). Arrhenius plots with these data yield the activation energy data assembled in Table VIII.

As can be seen, a strain effect superimposes to temperature, so that the larger the strain amplitude, the lower the activation energy for a given compound. Furthermore, the highly filled material exhibits significantly lower activation energy values; an observation that might be related at first sight to the considerable difference between the specific heat capacities of the filler and the rubber matrix (respectively, 0.913 for carbon black vs. 2.1 J/g.K for SBR1500), although the exact reasons are likely more

TABLE VIII
Filled SBR Compounds: Activation Energy for G^* (at 0.5 Hz) at Various Strain Amplitudes

	Activation energy (kJ/mole)		
SBR compound	For G^*_0	For G^*_{md}	For G^*_{600}
No black	16.30	14.91	11.75
10 phr N330	17.54	16.23	12.45
50 phr N330	10.55	9.94	11.09

complex. As above, normalized fitted curves clearly illustrate this behavior (Fig. 8).

The additional nonlinearity imparted by the filler is clearly appearing in such graphs. At low carbon black content, i.e., 10 phr (or 0.043 volume fraction, largely below the so-called percolation level of 13%), the overall behavior is essentially the one of the rubber matrix and, as observed with the gum SBR, a strain effect superimposes to the temperature one, but they are factorable only in the linear viscoelastic region. A reinforcing filler like carbon black amplifies these combined effects, further complicated by the essential nonlinear character of such a complex polymer system that, amongst other results, moves the linear viscoelastic region (if any) to very low strain amplitudes, clearly out of reach of the experimental window. How carbon black does bring an additional nonlinear character to rubber compounds is not yet clearly understood but a number of available theoretical considerations assign a key role to specific interactions between filler particles and the neighboring part of the rubber matrix (see Ref. 21 for a review and discussion of recent theoretical proposals).

It is worth noting that the above observations are somewhat qualitatively conform to long reported results on disperse systems consisting of concentrated solutions of polymers with various levels and types of fillers. For instance Onogi et al.[22] assessed the nonlinear viscoelasticity of concentrated solutions of 80 wt % polystyrene in diethyl phthalate with various levels (0, 20, 25, and 30 wt %) of 40 μm average diameter carbon black particles, by means of a torsional oscillating Couette rheometer. Using a Fourier Transform approach to obtain the fundamental as well as the second, third, and higher order harmonics, they found that the nonlinearity became more important with higher filler loading, and that the temperature dependence reduced with increasing temperature. With the same coaxial cylinder rheometer and method of analysis, Matsumoto et al.[23] studied the effect of temperature on both the linear and nonlinear viscoelastic shear moduli of 20 wt % solutions of polystyrene in diethyl phthalate loaded with various amounts (5, 10, and 20 wt %) of solid PS particles crosslinked by divinylbenzene. Such particles were uniform spheres of around 200 nm. These authors reported that both the linear and nonlinear functions (i.e., vs. frequency) at fixed strain of 26% become less sensitive to temperature as temperature rises (in the 10–70°C range). Both the linear and the nonlinear viscoelastic functions, at any investigated frequency, were found to decrease with increasing strain amplitude but the strain span considered (10.7 to 39%) was clearly insufficient to document the overall linear-to-nonlinear range.

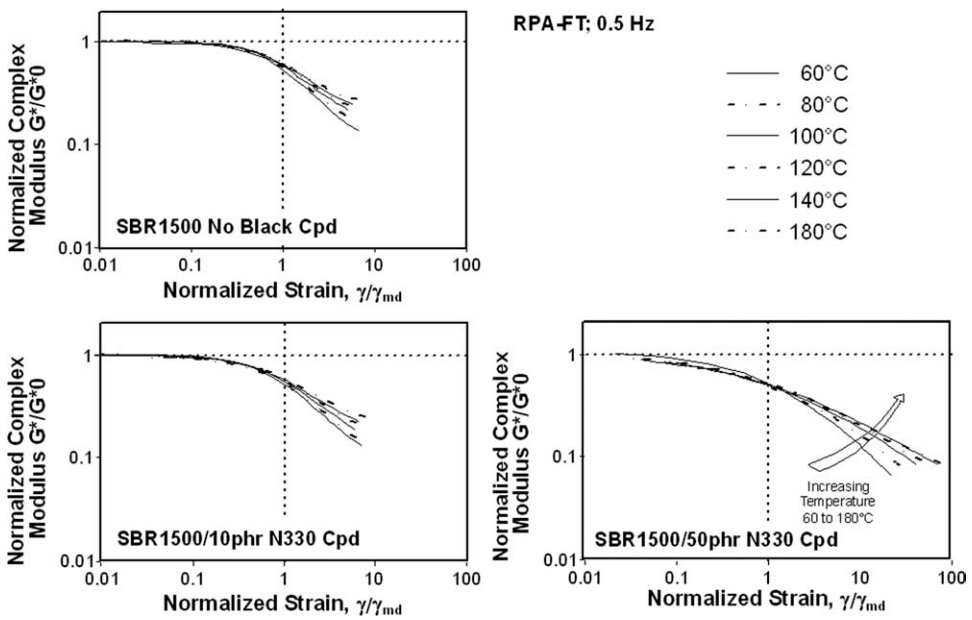

Figure 8 Normalized complex modulus vs. strain curves at various temperatures for carbon black filled SBR compounds.

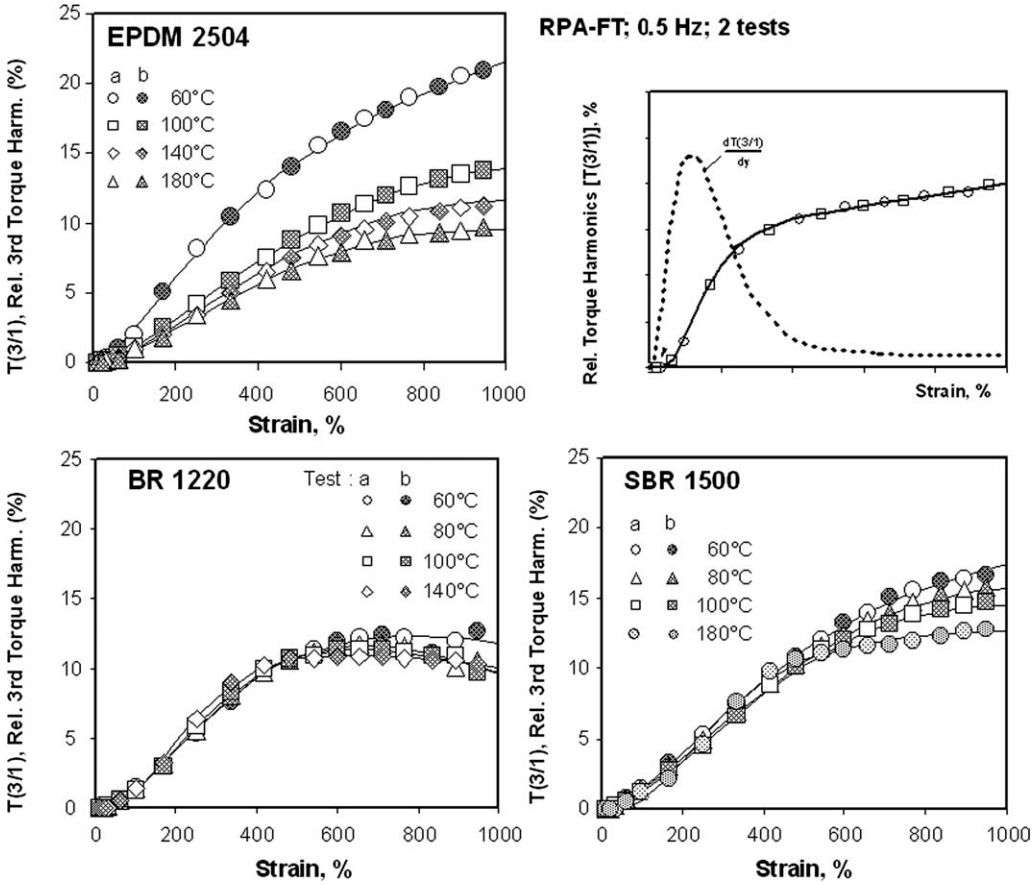

Figure 9 Third relative torque harmonic vs. strain amplitude as measured of gum rubber samples at various temperatures.

Gum rubber: Third relative torque harmonic variation with strain amplitude and temperature

As shown in Figure 3 above, the nonlinear viscoelastic signature of polymer systems can be safely investigated with our rheometer by considering the third, the fifth, and the sum of all odd harmonics up to the 15th. In all case, fitting experimental data with eq. (2) generally gives excellent results. In this report, we will however restrict the analysis and the discussion to the third relative torque harmonic, the most intense one. Figure 9 displays selected TH(3/1) vs. strain amplitude data as measured on the three gum rubber samples at various temperatures. Curves were drawn with fit parameters reported in Table V.

As can be seen, the three rubber samples are quite different in what the evolution of their nonlinear character with temperature is concerned. BR 1220 shows no significant effect of temperature in the linear-to-nonlinear transition region, i.e., approximately up to 500% strain amplitude. In the high-strain region, the lower the test temperature the higher the third relative harmonic but eq. (2) looses some applicability and/or there is a larger scatter. EPDM 2504 exhibits a nonlinear viscoelastic signature that is significantly dependent on temperature at all strain amplitudes investigated, whereas SBR 1500's third torque harmonic is essentially affected by temperature in the large strain amplitude region, i.e., above 500%. The magnitude and position of the maximum of the first derivative of eq. (2) allow quantifying such differences, as shown in Figure 10.

As reported above (section 3.2.1) normalized complex modulus vs. strain curves superimpose at all tested temperatures for BR 1220 whereas third torque harmonic does not exhibit a strong temperature dependency with this material. Temperature sensitivity of normalized G^* curves in the high-strain region (i.e., beyond γ_{md}) is observed with EPDM and SBR, as well as a significant temperature of third torque harmonics for these polymers. Because torque harmonics are usually considered respective to the main torque harmonic (i.e., at the applied frequency), it is quite obvious that any temperature effect on the latter somewhat complicates the temperature dependence of the former. Results reported above suggest however that the main torque component (or the complex modulus) and the odd harmonics might not share the same temperature dependency at all strain amplitudes, with the chemical nature of the polymer playing a key role. More

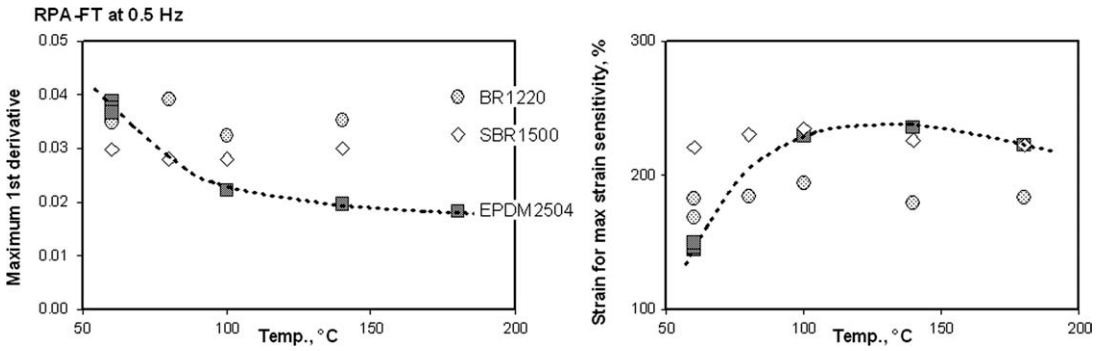

Figure 10 Gum rubbers; magnitude and position of the first derivative of TH(3/1) vs. strain curves; note that dashed lines for EPDM2504 are loose curves to guide the eye. Note that experiments on EPDM2504 were performed three times at 60°C to confirm data points.

results with a broader range of different elastomers are necessary to fully document this aspect.

In the cases of BR and SBR, both the maximum strain sensitivity (i.e., maximum first derivative) and its position seem to slightly increase with increasing temperature, EPDM 2504 exhibits a more complex behavior with significant effects of test temperature.

Filled rubber compounds: Third relative torque harmonic variation with strain amplitude and temperature

Figure 11 shows typical third relative torque harmonic data as measured on carbon black filled SBR compounds, and the magnitude and position of the first derivative of TH(3/1) vs. strain curves. In all cases (unfilled or filled compounds), eq. (3) gives excellent to reasonably good fits of experimental data over the whole strain range investigated. Depending on the filler content and the test temperature, the additional nonlinearity imparted to compounding ingredients (with the filler playing the major role) is more or less appearing. Such a behavior was previously reported with natural rubber compounds loaded with high levels of reinforcing grades of carbon black.[8] This results further demonstrate that adding extra terms to eq. (2) to obtain eq. (3) is a very convenient manner to consider the effect of a strain-sensitive filler network on the variation of torque harmonics with strain amplitude.

Once experimental data have been well fitted with a convenient model, then exploiting the mathematical virtues of the model leads to a thorough discussion of the strain and temperature effects. For instance, the magnitude and position of the first derivative of eq. (3), are worth consideration because they document the maximum strain sensitivity region. As shown in the bottom graphs of Figure 11, the position of the maximum of the first derivative tends to decrease with increasing temperature but the filler effect is much larger that the temperature's one. Indeed with respect to the "no black" compound, adding 50 phr carbon black moves back the position of maximum of the first derivative by some 100%, whereas the reduction because of an increase of 100°C is around 10–15%. Such an observation is of course in line with the severe reduction of the extent of the linear region as filler loading increases, as discussed in section "Filled compounds: complex modulus variation with strain amplitude and temperature" above. The magnitude of the first derivative (bottom right graph) provides additional information. Indeed, the unfilled and low filled compounds exhibit a nearly identical and constant value, whatever is the temperature, but the 50 phr black compound shows a maximum of the first derivative that clearly increases with temperature. In other words, with a highly filled compound, the higher the temperature, the stepper the TH(3/1) vs. strain curve in the transition region. This effect is due to the complex network of rubber-filler particles that controls the dynamic strain response of the material until the strain is large enough for this network to be dislocated. The higher the temperature the faster the dislocation process is. It is worth noting that this observation is well in line with the severe decrease in bound rubber, once the temperature exceeds a certain level, as reported by Wolff et al.[24] It follows that at high temperature, the large strain dynamic behavior of a (unvulcanized) carbon black filled compound is likely to be essentially controlled by the rubber matrix.

How the W_i parameters of the filler component of eq. (3) vary with temperature is also worth consideration. Indeed (Table VI), W_3 is constant and equal to around 3.05 for all samples at all test temperatures. For the unfilled and the 10 phr carbon black filled compound, W_1 and W_2 are very similar; the former decreases with increasing temperature but the latter is nearly not affected by temperature (Fig. 12). The highly filled compound exhibits contrasting trends: both W_1 and W_2 increase with increasing temperature. Such observations are somewhat supporting the physical interpretation of these parameters. Indeed

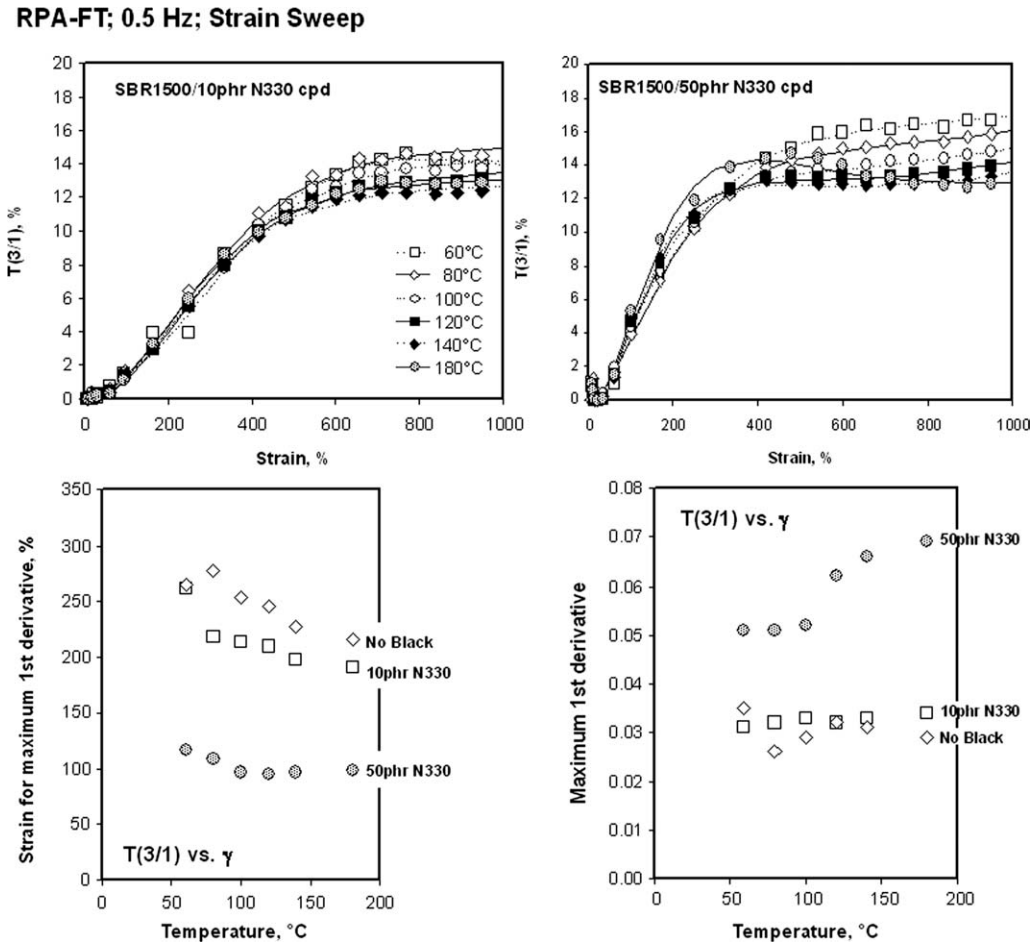

Figure 11 Typical nonlinear viscoelastic signatures of carbon filled SBR compounds as measured at different temperature. Upper curves were drawn with eq. (3) and fit parameters in Table VI. The lower left graph displays the strain for the maximum of the first derivative of eq. (3) and the right lower graph shows the maximum of the first derivative.

below a critical level (generally considered to be close to the theoretical percolation volume of 13%) reinforcing fillers do not change much the rheological properties of compounds. At best an increase, proportional to filler loading, of rheological quantities such as the viscosity or the dynamic moduli is observed but the shape of rheological functions remains essentially unchanged. If the reinforcing character of the filler is reflected by W_1 and W_2 then no much difference is expected between an unfilled and a slightly loaded compound, as indeed observed. With filler volume above the percolation level, a

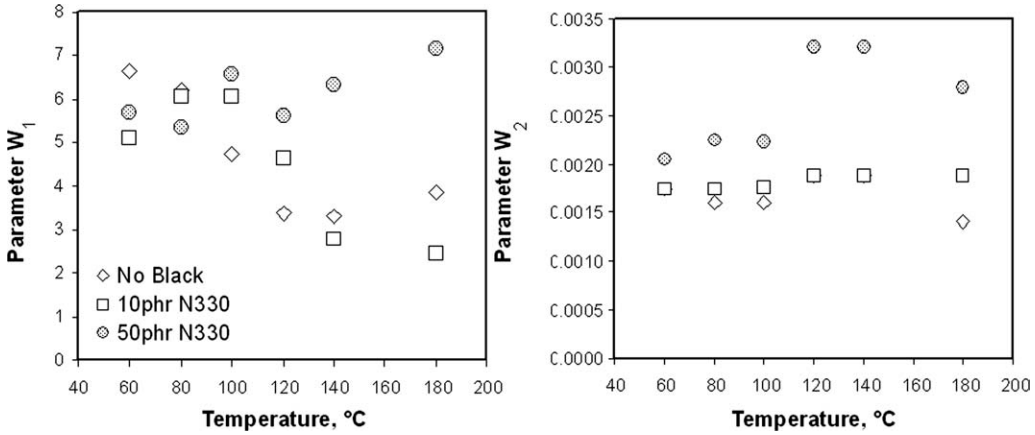

Figure 12 Variation of the filler component parameters in eq. (3) with both filler level and temperature.

complex network develops through interactions between filler particles and the rubber matrix. Parameter W_1 is reflecting the response of this complex filler-rubber network to dynamic strain and this explains the sharp contrast between the response of the unfilled (or low filled) and the highly filled materials. However, the fact that, once the filler level is sufficiently high, both W_1 and W_2 increase with higher temperature might be considered as an indication that the additional viscoelastic nonlinearity exhibited by filled materials is mainly due to the polymer that interacts with filler particles.

CONCLUSIONS

Appropriate SS test protocols and the associated data treatments were successfully developed for a closed cavity torsional dynamic rheometer, to investigate the effect of test temperature when assessing dynamic properties in the linear and the nonlinear viscoelastic domains. Fourier Transform was used to extract valuable data from recorded strain and torque signals. SS tests (on two samples) last some 6 hours for five probed temperatures but yield a number of very sensible information.

As expected, the temperature dependency of the complex modulus G^* at any strain amplitude is conveniently considered by drawing Arrhenius plots to derive the activation energy, E_a. Either with unfilled elastomers or with carbon black filled compounds, it is observed that different E_a values govern the G^* vs. temperature variations in the linear and the nonlinear domains. Normalizing G^* vs. strain data with respect to the modulus in the linear region and with respect to the critical strain that corresponds to mid modulus allows data collected at different temperatures to collapse on a single curve in the linear domain. In the nonlinear domain, this normalization is not always sufficient to encompass strain magnitude effects. This implies that strain-temperature effects are not factorable in nonlinear viscoelasticity. The (chemical) nature of the rubber and the content of the filler are however key aspects of the combined strain-temperature effects in the nonlinear domain. For a given material, the manner the complex modulus varies with temperature provides a picture that must be completed by considering how torque harmonics varies with temperature.

As demonstrated, a set of relatively simple equations allows well fitting experimental data from dynamic SS experiments. Apart from the immediate benefit that a large number of data can be adequately summarized with a limited number of parameters, such a treatment of dynamic results yields quantities whose physical meaning helps understanding certain rheological aspects. This advantage is particularly interesting in what torque harmonics are concerned.

References

1. White, J. L. Rubber Chem Tech 2009, 82, 131.
2. Leblanc, J. L. Rubber Chem Tech 2010, 83, 65.
3. ASTM. Standard Test Methods for Rubber—Viscosity, Stress Relaxation, and Pre-Vulcanization Characteristics (Mooney Viscometer), ASTM D1646-03. ASTM International, West Conshohochen, PA, 2004; available at www.astm.org.
4. Rubber, Unvulcanized—Determinations Using a Shearing-Disc Viscometer—Parts 1, 2, 3, and 4: Determination of Mooney Viscosity, International Standards Organization, Geneva, Switzerland, 289-1:1994, available at www.iso.org.
5. ASTM. Standard Test Method for Rubber Property-Vulcanization Using Oscillating Disk Cure Meter, ASTM International, West Conshohochen, PA, 2004; D2084-07, available at www.astm.org.
6. ISO. Rubber—Measurement of Vulcanization Characteristics with the Oscillating Disk Rheometer, International Standards Organization, Geneva, Switzerland, available at www.iso.org, 3417.
7. ASTM D5289-07 –Standard Test Method for Rubber Property-Vulcanization Using Rotorless Cure Meters, ASTM International, West Conshohochen, PA, 2004; available at www.astm.org.
8. Friedrich, C.; Mattes, K.; Schulze, D. Non-Linear Viscoelastic Properties of Polymer Melts as Analyzed by LAOS-FT Experiments—IUPAC Macro 2004, Paris, France, July 4–9, paper 6.1.3.
9. Leblanc, J. L; Mongruel, A. Prog Rubb Plast Technol 2001, 17, 162.
10. Debbaut, B.; Burhin, H. J Rheol 2002, 46, 1155.
11. Leblanc, J. L.; de la Chapelle, C. Rubber Chem Tech, 2003, 76, 979.
12. Giacomin, A. J.; Dealy, J. M. In Rheological Measurements, 2nd ed.; Kluwer Academic Publishers: Dordrecht, Netherlands, 1998; Chapter 11, p 327.
13. Hyun, K.; Wilhelm, M.; Klein, C. O.; Cho, K. S.; Nam, J. G.; Ahn, K. H.; Lee, S. J.; Ewoldt, R. H.; McKinley, G. H. Prog Polym Sci 2011, 36, 1697.
14. Leblanc, J. L. J Rubber Res 2007, 10, 63.
15. Leblanc, J. L. J Appl Polym Sci, 2008, 109, 1271.
16. Wilhelm, M.; Maring, D.; Spiess, H. W. Rheol Acta 1998, 37, 399.
17. Leblanc, J. L. Prog Polym Sci 2002, 27, 627.
18. Arrhenius, S. Ph.D. Dissertation. Stockholm, Royal publishing house, P.A. Norstedt & Söner, 1884.
19. Ferry, J. D.; Child, W. C., Jr.; Zand, R.; Stern, D. M.; Williams, M. L.; Landel, R. F. J Colloid Sci 1957, 12, 53.
20. Plazek, D. J. J Phys Chem 1965, 69, 3480.
21. Leblanc, J. L. Filled Polymers: Science and Industrial Applications, CRC Press, Taylor & Francis Group: Baton Rica, FL, 2010; Chapter 5, ISBN 978-1-4398-0042-3.
22. Onogi, S.; Masuda, T.; Matsumoto, T. Trans Soc Rheol 1970, 14, 275.
23. Matsumoto, T.; Segawa, Y.; Warashina, Y.; Onogi, S. Trans Soc Rheol 1973, 17, 47.
24. Wolff, S.; Wang, M.-J.; Tan, E.-H. Rubber Chem Tech, 1993, 66, 163.